IL NUOVO CIMENTO Vol. 34 C, N. 2 Marzo-Aprile 2011
DOI 10.1393/ncc/i2011-10830-1

Colloquia: WISH2010

Jet conversion and quark coalescence in relativistic heavy-ion collisions

Che Ming Ko

Cyclotron Institute and Department of Physics and Astronomy, Texas A&M University College Station, TX 77843-3366, USA

(ricevuto il 10 Novembre 2010; approvato il 24 Dicembre 2010; pubblicato online il 16 Marzo 2011)

Summary. — One of the most interesting conclusions from the experimental results in relativistic heavy-ion collisions is that quark and gluon jets produced in initial hard scattering tend to lose significant amount of energies in the produced quark-gluon plasma, leading to the suppressed production of high transverse momentum hadrons. Model studies have indicated that energetic jets traversing the quark-gluon plasma not only lose their energies but also can undergo conversions between gluon and quark jets as well as between quark jets of different flavors. The resulting net conversion of quark to gluon jets reduces the difference between the nuclear modification factors for quark and gluon jets in central heavy-ion collisions and thus enhances the ratio of produced protons and pions at high transverse momenta. Furthermore, as jets leave the quark-gluon plasma, they can be converted to hadrons by coalescing with partons in the quark-gluon plasma, leading to an enhanced production of hadrons of intermediate transverse momenta. Comparisons of results from these model studies with experimental data from the Relativistic Heavy-Ion Collider (RHIC) and predictions for heavy-ion collisions at the Large Hadron Collider (LHC) are presented.

PACS 12.38.Mh – Quark-gluon plasma.
PACS 25.75.-q – Relativistic heavy-ion collisions.

1. – Introduction

In relativistic heavy-ion collisions, hadrons with large transverse momenta are from the fragmentation of quark and gluon jets produced in initial hard scattering of incoming nucleons by combining with quarks and antiquarks from the vacuum. Their suppressed production has been attributed to the radiative energy loss of partonic jets as they traverse the dense partonic matter created during these collisions [1-3]. More recently, it was realised that the elastic scattering of jets with partons in the partonic matter could also have non-negligible effects on their energy losses [4, 5]. Because of its larger color charge, a gluon jet is expected to lose more energy than quark and antiquark jets.

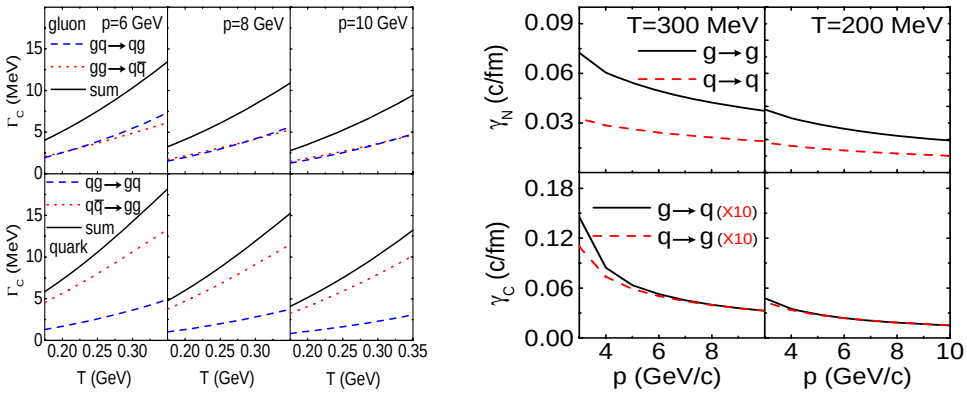

Fig. 1. – (Color online) Collisional widths (left window) and drag coefficients (right window) of quark and gluon jets due to $2 \to 2$ processes in a quark-gluon plasma.

Since the ratio of high-momentum protons and antiprotons to pions produced from the fragmentation of a gluon jet is much larger than that from a quark jet, a larger energy loss of gluon jets than that of quark jets would lead to smaller p/π^+ and $\bar{p}/\pi^-$ ratios at high transverse momenta in central heavy-ion collisions than in proton-proton collisions at same energy [6]. Experimentally, data from the STAR Collaboration have indicated, however, that both p/π^+ and $\bar{p}/\pi^-$ ratios at high transverse momenta in central Au + Au collisions [7] are similar to those in $p + p$ and $d +$ Au collisions [8]. This result implies that the ratio of final quark and gluon jets of high transverse momenta is similar to that of initially produced ones. A possible mechanism for reducing the effect due to different quark and gluon jet energy losses in the quark-gluon plasma (QGP) is to allow the conversion between quark and gluon jets via elastic $gq(\bar{q}) \to q(\bar{q})g$ and inelastic $q\bar{q} \leftrightarrow gg$ scattering with thermal quarks and gluons in QGP as shown in ref. [9].

2. – Jet conversion rates and drag coefficients in quark-gluon plasma

The conversion rate of a quark jet to a gluon jet or vice versa in a QGP is given by the collisional width $\Gamma_C = \sum_i \langle \overline{|\mathcal{M}_i|^2} \rangle / \hbar$, where the sum is over the conversion processes with $\overline{|\mathcal{M}_i|^2}$ being their squared amplitudes after averaging over the spins and colors of initial partons and summing over those of final partons. The symbol $\langle \cdots \rangle$ denotes average over the distributions of scattered thermal partons in the QGP and integration over the momenta of all final-state partons. Medium effects can be taken into account by using the thermal masses $m_q = m_g/\sqrt{3} = gT/\sqrt{6}$ [10] for quarks and gluons, where T is the temperature of the QGP and $\alpha_s = g^2/4\pi = 0.3$ is the QCD coupling constant. The resulting collisional widths for gluon to quark jet (upper panels) and quark to gluon jet (lower panels) conversions in a chemically equilibrated QGP are shown in the left window of fig. 1 for jets of momentum 6 (left panels), 8 (middle panels), and 10 (right panels) GeV/c. Because of the larger (about a factor of two) quark than gluon densities in the chemically equilibrated QGP with thermal quark and gluon masses, contributions from elastic (dashed lines) and inelastic (dotted lines) scattering to conversion of gluon jets to quark jets are comparable. For the quark to gluon jet conversions, inelastic scattering is, however, more important than elastic scattering. Adding both contributions leads to a larger total collisional width for the quark to gluon jet conversion than for the gluon to quark jet conversion, particularly at high transverse momenta.

The momentum degradation of a quark or gluon jet in a QGP depends on its drag coefficient, which is given by averages similar to that for the collisional width, *i.e.* $\gamma(|\mathbf{p}|,T)=\sum_i\left(\langle\overline{|\mathcal{M}_i|^2}\rangle-\langle\overline{|\mathcal{M}_i|^2}\mathbf{p}\cdot\mathbf{p}'\rangle/|\mathbf{p}|^2\right)$ where $\mathbf{p}$ and $\mathbf{p}'$ are, respectively, momenta of the jet before and after a collision. The quark and gluon drag coefficients evaluated with thermal quark and gluon masses and the QCD coupling $\alpha_s=0.3$ are shown in the right window of fig. 1 by dashed and solid lines, respectively, for non-conversion $2\to2$ (upper panels) and conversion $2\to2$ (lower panels) scatterings. It is seen that non-conversion scatterings generally lead to much larger drag coefficients than those from conversion scatterings. The effect of the more important radiative energy loss can be mimicked by introducing a phenomenological multiplication factor K_E. It was then found in ref. [9] that with $K_E=4$ both the values and transverse momentum dependence of resulting gluon and quark drag coefficients were comparable to those extracted from the energy loss formula derived in ref. [2] based on radiative scatterings of quark and gluon jets in the quark-gluon plasma.

3. – Nuclear modification factors for quark and gluon jets

A quark or gluon jet moving through a QGP changes its mean transverse momentum $\langle p_T\rangle$ according to the rate $\mathrm{d}\langle p_T\rangle/\mathrm{d}\tau=-\langle\gamma(p_T,T)p_T\rangle\approx\gamma(\langle p_T\rangle,T)\langle p_T\rangle$ [9]. Because of conversion scattering, the quark or gluon jet can be converted to a gluon or quark jet with a rate given by corresponding collisional width. The initial p_T spectra of quark and gluon jets in heavy-ion collisions at midrapidity have the form of an inverse power law, *i.e.*

$$\frac{\mathrm{d}N_i}{\mathrm{d}^2p_T}\approx\frac{A_i}{\left(1+\frac{p_T}{B_i}\right)^{\alpha_i}},\qquad i=q,\bar{q},g, \tag{1}$$

with A_i, B_i and α_i being constants, as obtained from multiplying the quark and gluon p_T spectra from the PYTHIA for $p+p$ collisions by the number of binary collisions in heavy-ion collisions, which is ~ 960 for central Au + Au collisions at center-of-mass energy $\sqrt{s_{NN}}=200\,\mathrm{GeV}$. In a simple fire-cylinder model [11], which assumes that the quark-gluon plasma formed in relativistic heavy-ion collisions evolves boost invariantly in the longitudinal direction but with an accelerated transverse expansion, the resulting nuclear modification factor R_{AA} for quark or gluon jets, defined by the ratio of their final to initial spectra, is shown in fig. 2. Upper and lower dash-dotted lines are, respectively, those for the quark and gluon jets using drag coefficients from two-body elastic scattering that are enhanced by the factor $K_E=4$ but without jet conversions. The smaller R_{AA} for gluons than for quarks is a result of their larger energy loss. Including conversions between quark and gluon jets through $2\to2$ conversion scattering reduces the difference between the quark and gluon R_{AA} as shown by dotted lines. The difference is further reduced if the conversion widths shown in the left window of fig. 1 are enhanced by a factor K_C. With $K_C=4$ (dashed lines), similar to the enhancement factor K_E for the quark and gluon drag coefficients, and larger, *e.g.*, $K_C=6$ (solid lines), the quark and gluon nuclear modification factors become even closer as shown, respectively, by dashed and solid lines in fig. 2.

The fact that the net quark to gluon jet conversion rate needed to obtain similar nuclear modification factors for quark and gluon jets is much larger than that given by the lowest-order QCD is not surprising as a similar enhancement factor is required for

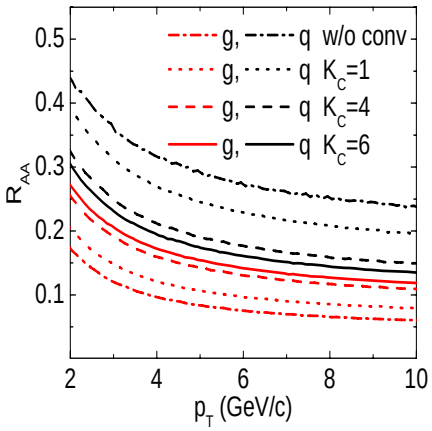

Fig. 2. – (Color online) Nuclear modification factor R_{AA} for quark (upper four lines) and gluon (lower four lines) jets in central Au + Au collisions at $\sqrt{s_{NN}} = 200\,\mathrm{GeV}$.

the drag coefficients of jets from the lowest-order QCD to describe their energy losses in QGP. Also, previous studies using the multi-phase transport (AMPT) model [12, 13], that includes only two-body scattering among partons, have shown that a much larger parton scattering cross-section than that given by the lowest-order QCD is needed to describe many other experimental observations at RHIC such as the large elliptic flows of hadrons made of light quarks [14, 15] or heavy quarks [16] and the two-pion correlation functions [17]. The large enhancement factor over the lowest-order QCD results can be considered as an effective parameter for taking into account effects not considered in ref. [9], such as higher-order contributions and multi-body scattering [18]. For example, higher-order $2 \to 3$ radiative scatterings with thermal partons in QGP, such as $gq \to qgg$, $g\bar{q} \to \bar{q}gg$, $q\bar{q} \to ggg$, and $gg \to q\bar{q}g$, can lead to similar quark and gluon jet conversion widths as the lowest-order two-body scatterings. Also, lattice QCD studies have shown that the QCD coupling constant at temperatures achieved at RHIC is larger than that given by the perturbative QCD, *i.e.*, $\alpha_s(T) = g^2(T)/4\pi \approx 2.1\alpha_{\mathrm{pert}}(T)$ [19]. The latter is consistent with the small viscosity needed in the hydrodynamic model [20-22] and the large parton scattering cross-sections used in the transport model [12, 13] to describe observed large hadron elliptic flow. The conversion widths for quarks and gluons using the larger in-medium QCD coupling $\alpha_s(T)$ result in quark and gluon nuclear modification factors in Au + Au collisions at $\sqrt{s_{NN}} = 200\,\mathrm{GeV}$ that are much closer to each other and also comparable to those obtained by multiplying the conversion enhancement factor $K_C = 4$ to the jet conversion widths calculated with the lowest-order $2 \to 2$ processes.

4. – Hadronization by fragmentation and coalescence

The effect of conversions between quark and gluon jets in QGP can be seen from hadrons produced from their fragmentation,

$$\frac{\mathrm{d}N}{\mathrm{d}^2\mathbf{p}_{\mathrm{had}}} = \sum_{\mathrm{jet}} \int \mathrm{d}z \frac{\mathrm{d}N}{\mathrm{d}^2\mathbf{p}_{\mathrm{jet}}} \frac{D_{\mathrm{had/jet}}(z, Q^2)}{z^2}\,, \tag{2}$$

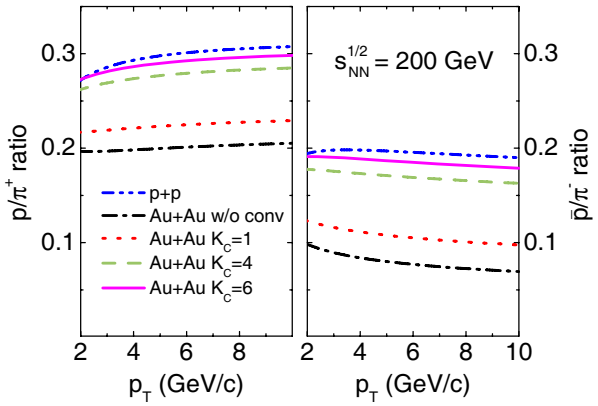

Fig. 3. – (Color online) The p/π^+ (left panel) and $\bar{p}/\pi^-$ (right window) ratios from quark and gluon jet fragmentation in central Au + Au collisions at $\sqrt{s_{NN}} = 200\,\mathrm{GeV}$. Data are from the STAR Collaboration [8].

where $z = p_{\mathrm{had}}/p_{\mathrm{jet}}$ is the fraction of jet momentum carried by the formed hadron and $Q = p_{\mathrm{had}}/2z$ is the momentum scale for the fragmentation process. The fragmentation function $D_{\mathrm{had/jet}}(z, Q^2)$ is usually determined empirically from hadron production in elementary collisions, and a frequently used one is the so-called AKK fragmentation functions [23]. The latter has been shown to reproduce the p/π^+ and $\bar{p}/\pi^-$ ratios at high transverse momenta in $p + p$ collisions. While protons and antiprotons are equally produced from gluon fragmentation, the fragmentation of quark and antiquark jets produce mainly protons and antiprotons, respectively [7, 8, 24]. Results for the p/π^+ and $\bar{p}/\pi^-$ ratios in central Au + Au collisions at $\sqrt{s_{NN}} = 200\,\mathrm{GeV}$ without jet conversions are shown by dash-dotted lines in fig. 3, and they are significantly below those in $p + p$ collisions. Including conversions between quark and gluon jets due to two-body elastic and inelastic scatterings increases p/π^+ and $\bar{p}/\pi^-$ ratios, as shown by dotted lines, but are still below those from $p + p$ collisions, which are shown by dash-dot-dotted lines. The p/π^+ and $\bar{p}/\pi^-$ ratios are further increased if quark and gluon jet conversions are enhanced by the factors $K_C = 4$ and 6 as shown by dashed and solid lines, respectively.

Because of the presence of the quark-gluon plasma in relativistic heavy-ion collisions, jets can also produce hadrons by coalescence or recombination with quarks and antiquarks in the quark-gluon plasma [25]. The number of mesons formed from the coalescence of jet quarks of phase-space distribution $f_q(x_1, p_1)$ with antiquarks of phase-space distribution $f_{\bar{q}}(x_2, p_2)$ in QGP is given by

$$E\frac{\mathrm{d}N_M}{\mathrm{d}^3\mathbf{p}_M} = g_M \int p_1 \cdot \mathrm{d}\sigma_1 p_2 \cdot \mathrm{d}\sigma_2 \frac{\mathrm{d}^3\mathbf{p}_1}{(2\pi)^3 E_1}\frac{\mathrm{d}^3\mathbf{p}_2}{(2\pi)^3 E_2} \times \delta^{(4)}(p_1 + p_2 - p_M) f_q(x_1; p_1) f_{\bar{q}}(x_2; p_2) f_M(x_1, x_2; p_1, p_2). \tag{3}$$

In the above, $\mathrm{d}\sigma$ denotes an element of a space-like hypersurface and g_M is the statistical factor that takes into account the internal quantum numbers in forming a colorless meson from spin-1/2 color quark and antiquark. The coalescence probability function $f_M(x_1, x_2; p_1, p_2)$, which depends on the overlap of the quark and antiquark wave functions with the internal quark and antiquark wave functions in the meson, is simply

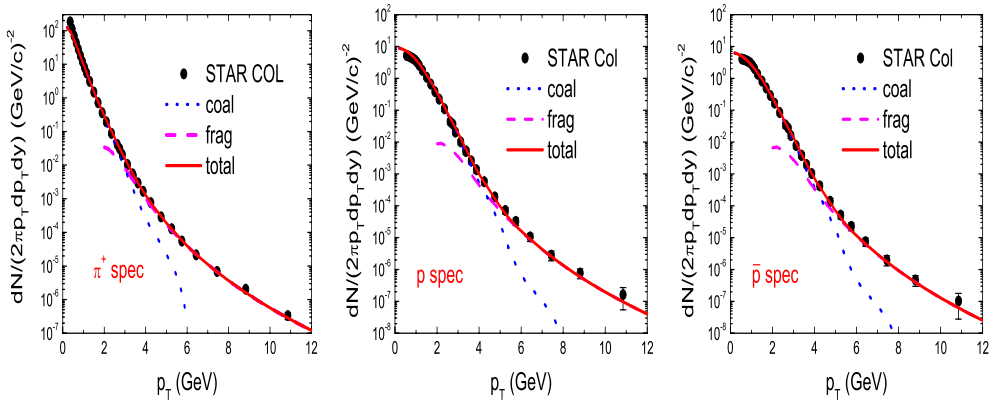

Fig. 4. – (Color online) Transverse momentum spectra of π^+ (left window), p (middle window), and $\bar{p}$ (right window) from quark coalescence (dotted lines), jet fragmentation (dashed lines), and their sum (solid lines). Data are from the STAR Collaboration [8].

the covariant meson Wigner distribution function that describes the probability for the quark and antiquark to have the relative coordinate $x_1 - x_2$ and the relative momentum $p_1 - p_2$. Equation (3) can be straightforwardly generalized to the production of baryons from the coalescence of quark jets with antiquarks in QGP. It can also apply to hadron production from coalescence among thermal quarks and antiquarks in QGP.

For thermal quarks and antiquarks in the midrapidity with strong Bjorken correlations, their phase space distribution at the phase transition temperature T_C, at which the coalescence occurs, is given by their p_T spectra,

$$\frac{\mathrm{d}N_{q,\bar{q}}}{\mathrm{d}^2 r_T \mathrm{d}^2 p_T} = \frac{g_{q,\bar{q}}^2 \tau_C m_T}{(2\pi)^3} \exp\left[-\frac{\gamma_T(m_T - p_T \cdot v_T) \mp \mu_b}{T_C}\right]. \tag{4}$$

In the above, $g_q = g_{\bar{q}} = 6$ are spin-color degeneracies of light quarks and antiquarks, respectively, v_T is the transverse flow velocity of the quark-gluon plasma, and $m_T = (m_{q,\bar{q}}^2 + p_T^2)^{1/2}$ is the transverse mass of quark or antiquark. The baryon chemical potential has the value $\mu_b = 10\,\mathrm{MeV}$ to give an antiproton to proton ratio of 0.7, consistent with the observed ratios at midrapiduty in heavy-ion collisions at RHIC. The masses of light quark and antiquark are taken to be $m_q = m_{\bar{q}} = 300\,\mathrm{MeV}$, similar to the masses of constituent quarks and antiquarks due to nonperturbative effects in the quark-gluon plasma near hadronization [26]. Equation (4) also applies to gluons after replacing $g_{q,\bar{q}}$ by the gluon spin-color degeneracy $g_g = 16$ and dropping the chemical potential. For the coalescence contribution to hadron production, both gluons in the QGP and gluon jets are converted to quarks and antiquarks of same momenta, with probabilities according to the flavor compositions in the quark-gluon plasma.

Including contributions of ρ, ω, and K^* decay to pion and of Δ decay to pion and proton, the transverse momentum spectra of π^+, p, and $\bar{p}$ from the quark coalescence are shown, respectively, by dotted lines in the left, middle, and right windows of fig. 4. Also shown by dashed lines are the spectra from the fragmentation of quenched jets. It is seen that the spectrum of pions with transverse momentum less than $3\,\mathrm{GeV}/c$ and those of protons and antiprotons with transverse momentum less than $4.5\,\mathrm{GeV}/c$ are dominated

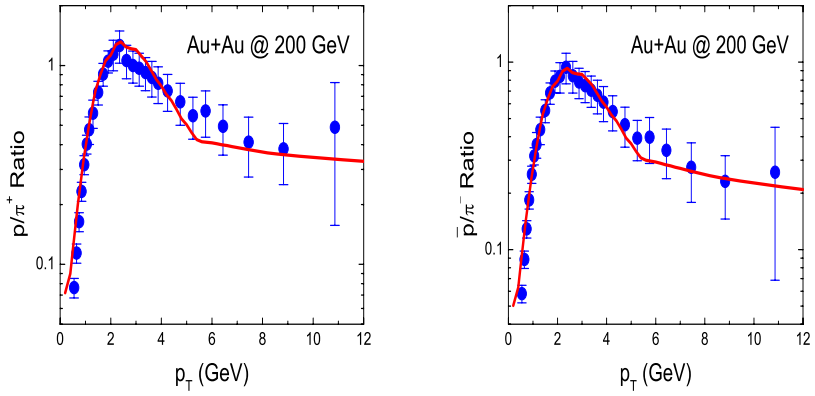

Fig. 5. – (Color online) The p/π^+ (left window) and $\bar{p}/\pi^-$ (right window) ratios including contributions from both quark coalescence and jet fragmentation. Data are from the STAR Collaboration [8].

by contributions from the quark coalescence. As shown in ref. [25], the coalescence of quark and gluon jets with those in QGP enhances the production of hadrons of intermediate momenta by a factor of about 2 and 5 for pions and protons, respectively. The total transverse momentum spectra including that from the jet fragmentation as shown by solid lines reproduce very well the measured ones (filled circles) from the STAR Collaboration [8]. The resulting p/π^+ and p/π^- ratios are shown by the solid line in the left and right windows of fig. 5, respectively, and they also agree with the experimental data very well except around $p_T = 5\,\mathrm{GeV}/c$, where a kink is seen in the ratio. The latter results from adding contributions from the two different mechanisms of quark coalescence and jet fragmentation, which have different momentum dependence with the former close to an exponential thermal spectrum while the latter being an inverse power law. Including rescattering of produced hadrons is expected to lead to smoother hadron spectra.

5. – Effects of jet conversions in QGP at LHC

For heavy-ion collisions at LHC, jet conversions are also expected to enhance the production of energetic protons [27], kaons, and photons [28]. The effect is, however, smaller than that in heavy-ion collisions at RHIC as a result of the larger ratio of gluon to quark jets at LHC. The predicted nuclear modification factors R_{AA} for π^+ and p at large transverse momenta in central Pb + Pb collisions at $\sqrt{s_{NN}} = 5.5\,\mathrm{TeV}$ at LHC are shown in the left window of fig. 6. It is seen that the R_{AA} of pions increases from 0.18 at $p_T = 5\,\mathrm{GeV}$ to 0.4 at $p_T = 40\,\mathrm{GeV}$ due to a smaller drag coefficient at large transverse momenta. The R_{AA} of protons has a similar behavior, but its value is smaller because of stronger suppression of gluon than quark jets. The resulting p/π^+ ratio with the inclusion of the jet conversion, shown by the solid line in the right window of fig. 6, approaches that in $p + p$ collisions at same energy (dashed line) when the transverse momentum becomes very large. At lower transverse momenta, the p/π^+ ratio in Pb + Pb collisions remains, however, smaller than that in $p + p$ collisions, which is different from that in heavy-ion collisions at RHIC as a result of the larger ratio of gluon to quark jets at LHC. Without conversions between quark and gluon jets, the p/π^+ ratio decreases by a factor of about two as shown by the dotted line.

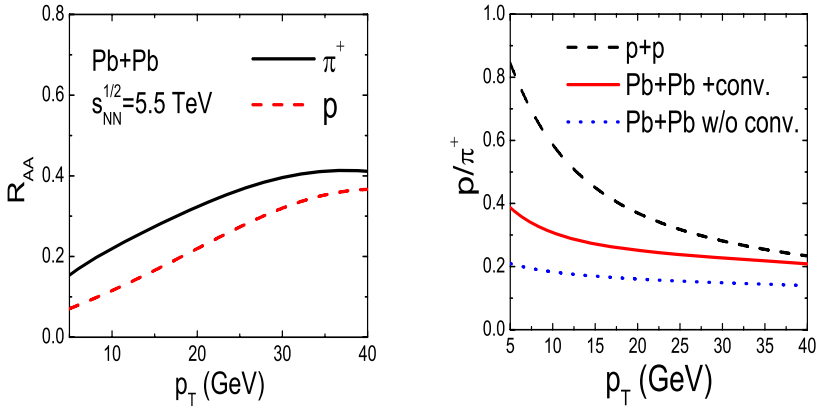

Fig. 6. – (Color online) Left window: nuclear modification factor R_{AA} for π^+ (solid line) and proton (dashed line) in central Pb + Pb collisions at $\sqrt{s_{NN}} = 5.5\,\text{TeV}$. Right window: p/π^+ ratio without (dotted line) or with jet conversions (solid line). The dashed line corresponds to $p + p$ collisions at same energy.

6. – Conclusions

Both elastic and inelastic two-body scatterings of quark and gluon jets in a quark-gluon plasma have effects not only on their energy loss but also on the conversions between them. Although inelastic two-body scatterings of quark-antiquark annihilation and gluon-gluon fusion always lead to conversions between quark and gluon jets, elastic two-body scatterings can be non-conversion scatterings if the momentum of the quark or gluon jet remains to be the one with a larger transverse momentum after the scattering. Two-body conversion scatterings lead to a small net conversion of the quark jets to the gluon jets, resulting in a slightly larger p/π^+ ratio compared to the case without conversions between gluon and quark jets but not large enough to bring the p/π^+ ratio in central Au + Au collisions to that of $p+p$ collisions at the same energy, as observed in experiments at RHIC. A large conversion enhancement factor of more than four, similar to that needed for the jet drag coefficients to describe the jet energy loss, is needed to explain the experimental observations. The large multiplicative factor over the lowest-order perturbative QCD cross-section can be considered as an effective parameter for taking into account the effects of higher-order contributions and multi-body scattering as well as the large QCD coupling constant at temperatures achieved at RHIC. Also, jet flavor conversions enhance the production of high momentum kaons and photons in heavy-ion collisions. Furthermore, the conversion between quark and gluon jets has been shown to be important for understanding both the large elliptic flow and the nearly equal nuclear modification factors of very high transverse momentum quarks and gluons in non-central heavy-ion collisions at RHIC [29]. For heavy-ion collisions at LHC, jet flavor conversions are also expected to affect the nuclear modification factors of pions and protons as well as their ratio. These studies have been based on the assumption that the QGP produced in heavy-ion collisions is in chemical equilibrium with about twice many massive quarks and antiquarks than massive gluons. If the produced partonic matter is a pure gluon matter, the resulting p/π^+ and $\bar{p}/\pi^-$ ratios in central Au + Au collisions turn out to be slightly smaller than those from a chemically equilibrated QGP as the gluon matter enhances the conversion of gluon jets to quark jets via the inelastic

scattering $gg \to q\bar{q}$. On the other hand, a pure quark and antiquark matter gives slightly larger p/π^+ and $\bar{p}/\pi^-$ ratios than from a chemically equilibrated QGP as the rate for the inelastic conversion process $q\bar{q} \to gg$ is enhanced. As for a chemically equilibrated QGP, none of these two scenarios is able to increase the p/π^+ and $\bar{p}/\pi^-$ ratios at high transverse momentum in central Au + Au collisions to approach those in $p + p$ collisions at same energy without a large enhancement factor for the net quark to gluon jet conversion rate.

* * *

This talk was based on a work supported in part by the U.S. National Science Foundation under Grant No. PHY-0758115 and the Welch Foundation under Grant No. A-1358.

REFERENCES

[1] Wang X. N., *Phys. Lett. B*, **579** (2004) 299.
[2] Gyulassy M., Lévai P. and Vitev I., *Phys. Rev. Lett.*, **85** (2001) 5535.
[3] Wiedemann U. A., *Nucl. Phys. B*, **588** (2000) 303.
[4] Mustafa M. G., *Phys. Rev. C*, **72** (2005) 014905.
[5] Wicks S., Horowitz W. Djordjevic M. and Gyulassy M., *Nucl. Phys. A*, **784** (2007) 426.
[6] Wang X. N., *Phys. Rev. C*, **58** (1998) 2321.
[7] Adams J. *et al.* (STAR Collaboration), *Phys. Rev. Lett.*, **97** (2006) 152301.
[8] Adams J. *et al.* (STAR Collaboration), *Phys. Lett. B*, **637** (2006) 161.
[9] Liu W., Ko C. M. and Zhang B. W., *Phys. Rev. C*, **75** (2007) 051901(R).
[10] Blaizot J. P. and Iancu E., *Phys. Rep.*, **359** (2002) 355.
[11] Chen L. W., Greco V., Ko C. M., Lee S. H. and Liu W., *Phys. Lett. B*, **601** (2004) 34.
[12] Zhang B., Ko C. M., Li B. A. and Lin Z. W., *Phys. Rev. C*, **61** (2000) 067901.
[13] Lin Z. W., Ko C. M., Li B. A., Pal S. and Zhang B., *Phys. Rev. C*, **72** (2005) 064901.
[14] Lin Z. W. and Ko C. M., *Phys. Rev. C*, **65** (2002) 034904.
[15] Chen L. W., Ko C. M. and Lin Z. W., *Phys. Rev. C*, **69** (2004) 031901(R).
[16] Zhang B., Chen L. W. and Ko C. M., *Phys. Rev. C*, **72** (2005) 024906.
[17] Lin Z. W., Ko C. M. and Pal S., *Phys. Rev. Lett.*, **89** (2002) 152301.
[18] Ko C. M. and Liu W., *Nucl. Phys. A*, **783** (2007) 233c; Liu W and Ko C. M., *J. Phys. G*, **34** (2007) S775; arXiv:nucl-th/0603004.
[19] Kaczmarek O., Karsch F., Zantow F. and Petreczky P., *Phys. Rev. D*, **70** (2004) 074505.
[20] Teaney D., Lauret J. and Shuryak E., *Phys. Rev. Lett.*, **86** (2001) 4783.
[21] Huovinen P., Kolb P. F. Kolb and Heinz U., *Nucl. Phys. A*, **698** (2002) 475.
[22] Hirano T. and Tsuda K., *Phys. Rev. C*, **66** (2002) 054905.
[23] Albino S., Kniehl B. A. and Kramer G., *Nucl. Phys. B*, **725** (2005) 181.
[24] Straub P. B. *et al.*, *Phys. Rev. D*, **45** (1992) 3030.
[25] Greco V, Ko C. M. and Lévai P., *Phys. Rev. Lett.*, **90** (2002) 202302; *Phys. Rev. C*, **68** (2003) 034904.
[26] Lévai P. and Heinz U., *Phys. Rev. C*, **57** (1998) 1879.
[27] Armesto N. *et al.*, *J. Phys. G*, **35** (2008) 054001.
[28] Liu W. and Fries R. J., *Phys. Rev. C*, **77** (2008) 054902.
[29] Scardina F., Di Toro M. and Greco V., *Phys. Rev. C*, **82** (2010) 054901.